

## COMPLEX RESISTIVITY RESPONSE OF A BURIED VERTICAL CYLINDRICAL BODY IN A HOMOGENEOUS EARTH

F.N. TROFIMENKOFF<sup>1</sup>, J.W. HASLETT<sup>1</sup>, R.H. JOHNSTON<sup>1</sup> AND A. KLASSEN<sup>1</sup>

### ABSTRACT

A line current source technique for modelling the effects of well casings on complex resistivity dipole-dipole surveys has been adapted to deal with buried cylindrical bodies of considerable radial extent. The calculations account for earth and buried body polarization effects and have been adapted to produce normalized resistivity magnitude and phase plots for simulated traverses. Parameters such as array size, spacing and location, body size and burial depth, earth and body complex resistivity, body surface impedance, etc. can be varied. Array mutual coupling can be included if desired.

### 1. INTRODUCTION

An efficient and accurate line current source modelling technique for dealing with a finite-length vertical cylindrical body such as a well casing in a homogeneous earth has been described in the literature (Johnston et al., 1987, 1992). More recently, the above method has been modified to deal with a buried vertical cylinder and to permit the use of a Cole-Cole model for the resistivity of the homogeneous earth (Trofimenkoff et al., 1993). In this work, a buried vertical cylinder with a resistivity that can also be described by a Cole-Cole model is considered in an attempt to determine the electromagnetic response of a geological formation such as a kimberlite pipe (Macnae, 1979) or a geochemical plume that may exist over a hydrocarbon deposit (Sternberg, 1991).

The line source calculational technique is also used here to model near-surface bodies of considerable spatial extent by using cylinder length/diameter aspect ratios as low as 3/2. Two examples of computations for such bodies have been drawn from the literature for comparison purposes. The first of these is the conducting square-ended vertical prism with end area " $a \times a$ " and height " $2a$ " located a distance " $a$ " beneath the surface discussed by Dey and Morrison (1979). A complex resistivity measurement with a collinear dipole-dipole array of dipole length " $a$ " and various dipole spacings " $na$ " has been simulated using a

personal computer program developed by the authors. The total time to run the program and to plot the results on a 50/25 MHz 486 personal computer with a math coprocessor was about 10 seconds (for 6 values of dipole separation and 50-point horizontal traverses). The results so obtained are sufficiently similar to those presented in the pseudo-section provided by Dey and Morrison (1979) to be useful for ascertaining detectability and depth. There are, however, significant anomaly shape differences, as might be expected, since the modelling technique can only be accurate for cylinders with diameters much smaller than the length.

The second of these examples is a spherical body of radius " $1.75a$ " buried a distance " $a$ " beneath the surface considered by Merkel and Alexander (1971). Again, a collinear dipole-dipole array measurement of the complex resistivity using a dipole length of " $a$ " and various dipole separations " $na$ " was simulated. Because the minimum number of line segments required to simulate any buried body is two, the resulting simulation of the sphere is not as satisfactory as that for the first example. Nevertheless, the results display anomaly-shape features similar to those given by Merkel and Alexander (1971) and the numerical values for the maximum response and the body depth are in relatively close agreement (total simulation and plotting time of 4 seconds for 6 values of dipole spacing and 50-point horizontal traverses).

The speed with which various analyses can be carried out and plotted allows experimentation that has heretofore not been possible. Array configuration and location, frequency, earth and cylinder resistivity, cylinder surface coating, cylinder permeability, cylinder diameter and length, depth of burial, etc., can all be varied to ascertain detectability and to interpret measured data. Array mutual coupling can be included or not as desired. Thus, the methods described by Johnston et al. (1987, 1992) and Trofimenkoff et al. (1993) together with the high-speed program that has been developed provide a valuable tool for both teaching and designing and interpreting field tests.

Manuscript received by the Editor April 6, 1995; revised manuscript received September 10, 1995.

<sup>1</sup>Department of Electrical and Computer Engineering, The University of Calgary, Calgary, Alberta T2N 1N4

This work was funded by the Natural Sciences and Engineering Research Council of Canada (NSERC) via Research Grants OGP0003382, OGP0007776 and OGP0007701.

2. CALCULATIONAL METHOD

As outlined in the literature by Johnston et al. (1987, 1992), a cylinder in a half-space can be modelled by initially considering a cylinder in a full space as shown in Figure 1. A full-space cylinder of length  $2l$  is modelled using  $M$  line current sources ( $M$  odd). The central  $N$  line current sources ( $N$  odd) can be deleted to model burial of a cylinder in a half-space as shown in Figure 2. The only other modification to the work outlined by Johnston et al. (1987, 1992) is the replacement of  $\rho$  and  $\rho_m$ , the half-space and cylinder dc resistivities, by Cole-Cole complex resistivities (Pelton et al., 1983) of the form, for example, for the earth,

$$\rho_{cc} = \rho \left[ 1 - m \left( 1 - \frac{1}{1 + (j\omega\tau)^c} \right) \right], \quad (1)$$

where  $\rho$  = zero frequency value of  $\rho_{cc}$ , ohm meters,

$m$  = chargeability,

$\tau$  = time constant, seconds,

$\omega$  = angular frequency, radians/second

and

$c$  = dispersion index.

Since line current source modelling is central to this work,

it is useful to consider the nature of the equipotentials around the line current source shown in Figure 3. In the plane of the diagram, the equipotential that passes through the point a distance "r" from the midpoint of the line current source can be traced out by noting that  $r_1 + r_2$  must be equal to  $2\sqrt{s^2 + r^2}$  (Wait, 1982). The full equipotential surface can then be traced out by revolving the prolate ellipsoid that results from the above construction method about the line current source. Modelling a traverse over a buried cylindrical body as shown in Figure 4 involves selecting  $M$ ,  $N$  and  $r$  and hence  $s = l/M$  to achieve the best possible coincidence of the equipotentials passing through  $r$  with the surface of the cylindrical body. The line source analysis procedure is then used to set up and solve equations for the strength of the line current sources by considering the potential at the surface of each ellipsoid developed by its own line current source, the line current source of every other ellipsoid, and by the surface array current sources. In carrying out the above analysis, longitudinal cylinder impedance, surface cylinder impedance and the requirement that there be no net current flow into the cylinder (or cylinders in the case of cylinder burial) must be considered as outlined in detail by Johnston et al. (1987, 1992).

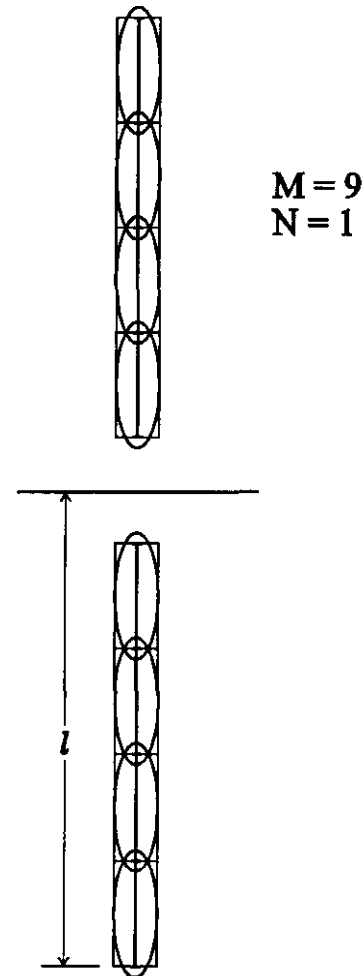
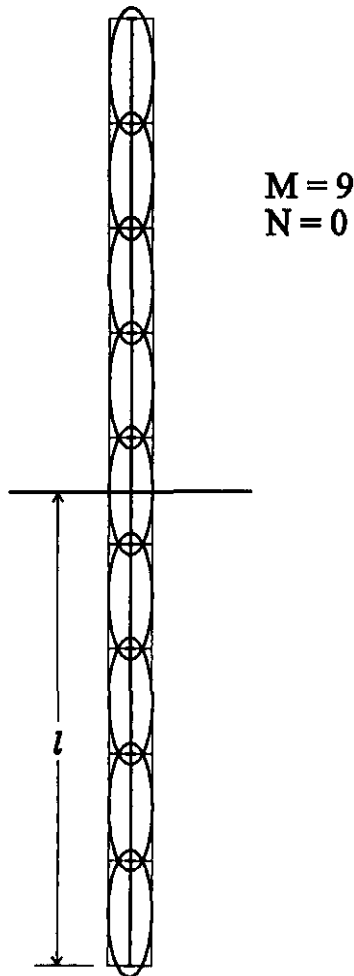


Fig. 1. Full space current source modelling of a cylinder,  $M$  sections in total.

Fig. 2. Full space current source modelling of a buried cylinder,  $M$  sections in total, middle  $N$  sections deleted.

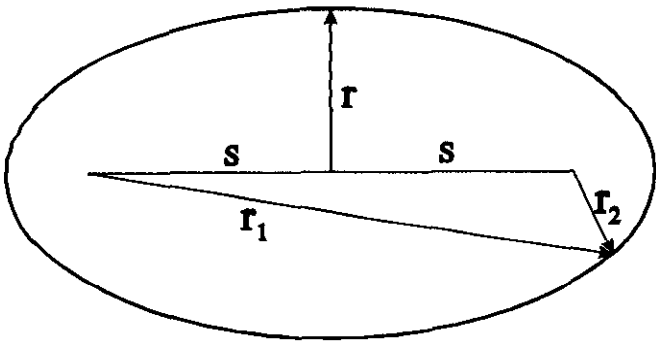


Fig. 3. Equipotentials around a line source of length  $2s$ .

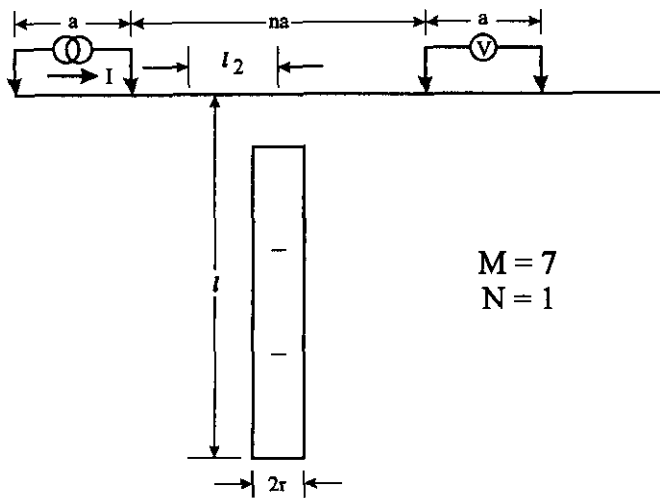


Fig. 4. Dipole-dipole traverse over an  $M = 7, N = 1$  example.

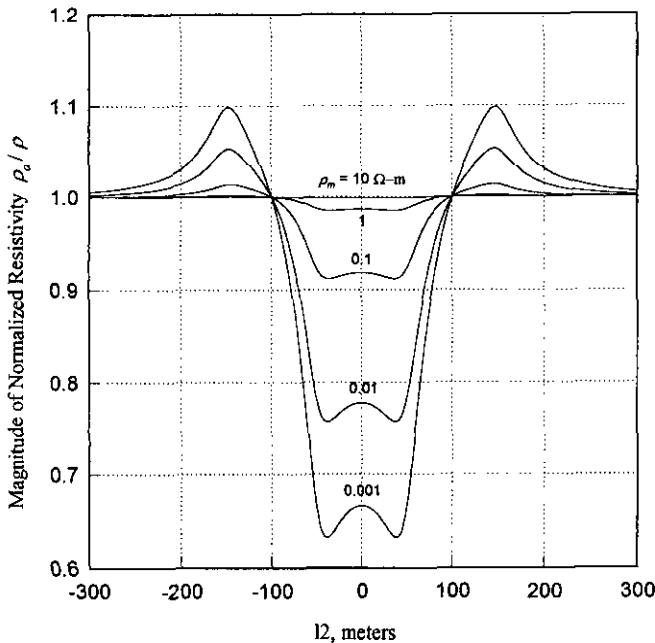


Fig. 5. Traverse directly over a solid cylinder of length 1010 metres, outer radius of 1 metre and various  $\rho_m$  values buried 10 metres below the surface;  $\rho = 100$  ohm metres,  $a = 100$  m,  $na = 100$  m, frequency = 1 Hz and earth and cylinder relative permeability = 1.0.  $M = 101, N = 1$ .

The validity of the calculational technique has been checked (Johnston et al., 1992) for a highly conducting cylinder with an outer radius "a" much smaller than a line current length  $2l / M$  by duplicating the results for an infinitely long cylinder which extends to the surface provided by Williams and Wait (1985). In the present work, thin buried cylinders with resistivities approaching that of the homogeneous half-space are considered first. For this case, cylinder burial is not expected to pose a problem because the equipotentials at the cylinder top and bottom only represent a rounding of the top and bottom ends of the cylinder (see Figure 2, for example). It is, however, necessary to demonstrate that simulations of dipole-dipole array complex resistivity measurements around a thin finite-length buried cylinder as shown in Figure 4, using the line source modelling technique, are sufficiently accurate to be usable when the resistivity contrast between the buried body and the host earth is small.

### 3. LONG, THIN CYLINDERS WITH $\rho_m \rightarrow \rho$ , NO INDUCED POLARIZATION

The results of simulations of dipole-dipole apparent complex resistivity surveys over 1010 metre-length solid vertical cylinders with 1 and 10 metre outer radii which are buried 10 metres below the surface are shown in Figures 5 and 6. The relative permeability of the cylinders has been taken to be unity and the cylinders have been assumed to be in perfect contact with a homogeneous earth with a resistivity of 100 ohm metres. An equispaced dipole-dipole array ( $n = 1$ ) with a dipole length of 100 metres has been traversed directly over the cylinders at a signal frequency of 1 hertz. The lowest

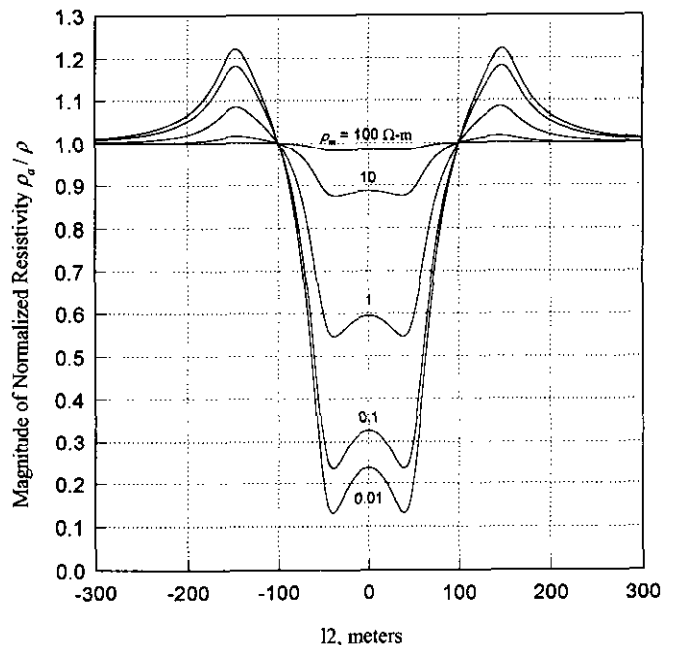


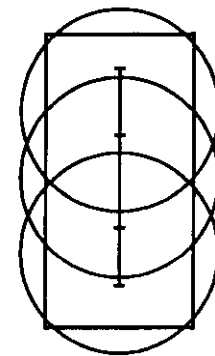
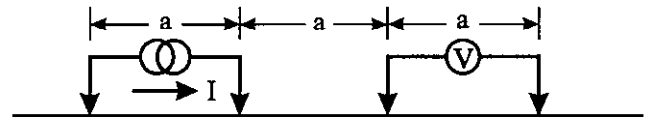
Fig. 6. Traverse directly over a solid cylinder of length 1010 metres, outer radius of 10 metres and various  $\rho_m$  values buried 10 metres below the surface;  $a = 100$  m,  $na = 100$  m, frequency = 1 Hz and earth and cylinder relative permeability = 1.0.  $M = 101, N = 1$ .

value of normalized apparent resistivity in Figures 5 and 6 is such that there is no substantial decrease in the normalized apparent resistivity as the resistivity of the cylinders,  $\rho_m$ , is decreased further. It is clear from Figure 5 (1 metre outer radius case) that there would be no practically detectable anomaly predicted by the model as  $\rho_m$  approaches  $\rho$ . The situation for the 10-metre outer radius cylinder of Figure 6 is, however, different. There is now a noticeable anomaly predicted by the model for  $\rho_m = \rho$ . If attention is focussed on  $\rho_m$  between 10 ohm metres and 100 ohm metres (see Figure 7), it is found that the maximum response predicted by the model for  $\rho_m = \rho$  is about 2% of the maximum response for  $\rho_m = 0.001$  ohm metres (see Figure 5) and about 15% of the maximum response for  $\rho_m = 10$  ohm metres. Clearly, some care would have to be exercised in interpreting results of simulations for  $\rho_m$  greater than  $0.1 \rho$ .

#### 4. THE DEY AND MORRISON EXAMPLE, NO INDUCED POLARIZATION

One way of establishing the lower limit of the length-to-diameter ratio of cylinders that can be modelled satisfactorily using the line source technique is by comparison of simulation results with more exact calculations available in the literature. Dey and Morrison's (1979) example of an "a x a" square-ended prism of height 2a located a distance "a" beneath the surface can be modelled using  $M = 11$  and  $N = 5$  reasonably satisfactorily as shown in Figure 8. The results of the simulation of a dipole-dipole traverse directly over the prism using a dipole length of "a" = 60 m and various dipole separations are shown in Figure 9 for  $\rho_m = 3$  ohm metres and  $\rho = 100$  ohm metres. These results, converted to pseudosection

format, can be compared with the pseudosection provided by Dey and Morrison (1979) as shown in Figure 10. It will be noted that the minimum  $\rho_a/\rho$  occurs for a dipole separation of  $3a$  and the minimum value of  $\rho_a/\rho$  is about 0.8 in both cases. The calculated anomaly is, however, appreciably narrower than that predicted by Dey and Morrison, i.e., the maximum response occurs for smaller "na" and the pull-up of the responses directly over the buried body for larger dipole separations is also less pronounced than that predicted by Dey and Morrison. This is to be expected, since the modelling procedure concentrates the effect of the buried body to its centre via the vertical line current sources.



$M=11$   
 $N=5$   
 $\rho = 100 \Omega \text{ m}$   
 $\rho_m = 3 \Omega \text{ m}$   
 $a = 60 \text{ m}$

Fig. 8. Model of Dey and Morrison's a x a x 2a prism buried "a" = 60 m below the earth's surface using  $M = 11$ ,  $N = 5$ .

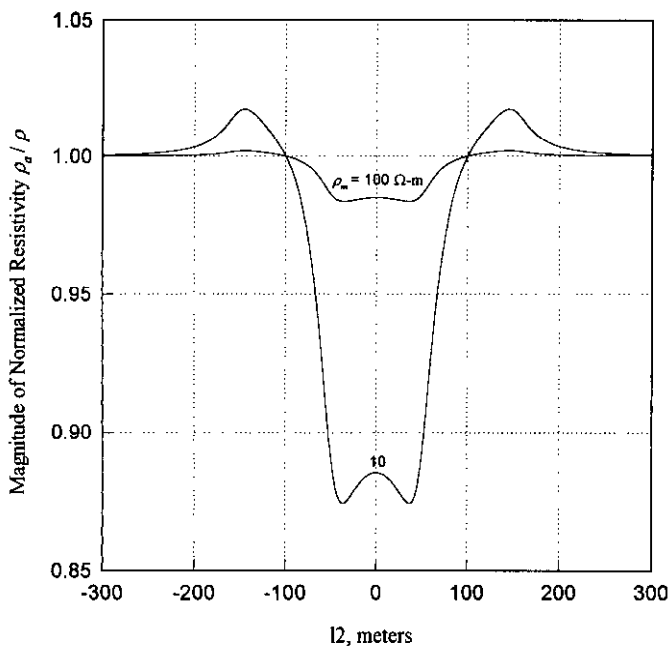


Fig. 7. Traverse directly over a solid cylinder of length 1010 metres, outer radius of 10 metres and various  $\rho_m$  buried 10 metres;  $a = 100$  m,  $na = 100$  m, frequency = 1 Hz and earth and cylinder relative permeability = 1.0.  $M = 101$ ,  $N = 1$ .

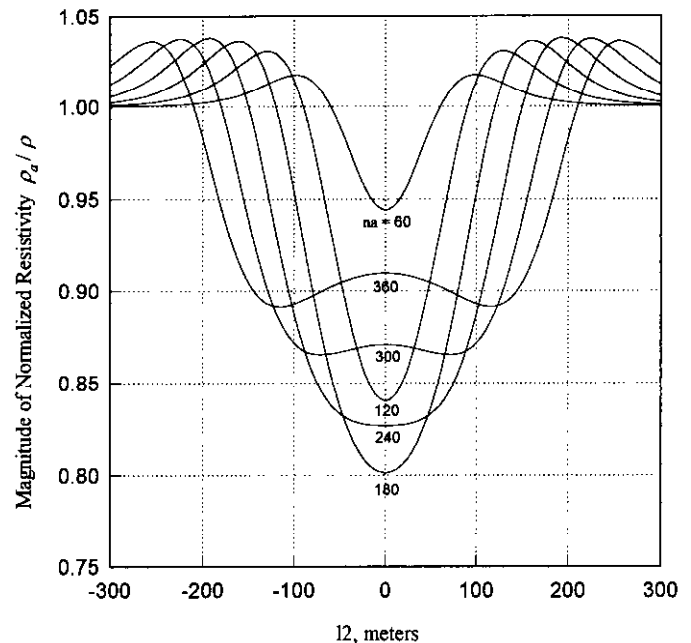


Fig. 9. Traverse directly over the prism of Figure 8 at a frequency of 1 Hz and earth and prism relative permeability of 1.0.



The magnitude of the anomaly predicted by the model for  $\rho_m \rightarrow \rho$  is illustrated in Figure 11 in which  $\rho_m$  is varied from 0.1 ohm metres to 100 ohm metres for a dipole separation of 3a. In this case, the maximum response for  $\rho_m = \rho$  is about 13% of the maximum response for  $\rho_m = 1$  ohm metre and 23% of the maximum response for  $\rho_m = 10$  ohm metres.

**5. THE MERKEL AND ALEXANDER EXAMPLE, NO INDUCED POLARIZATION**

The minimum value of (M-N) that can be used in the line source modelling method is 2 so that an attempt to model Merkel and Alexander's example of a 0.004 ohm-metre sphere of radius 1.75a buried a distance "a" = 9 m below the surface of a uniform earth of resistivity 1 ohm metre provides a fairly approximate simulation of the physical situation. Nevertheless, the results of a simulation of a dipole-dipole apparent resistivity traverse directly over the top of the ellipsoids of Figure 12 for a number of values of dipole separation are presented in Figure 13 for comparison with Merkel and Alexander's pseudosection of Figure 14. The maximum response for the M = 5, N = 1 model is about the same as in Merkel and Alexander's case but the pseudosection "depth" at which the maximum response occurs is greater, as would be expected. The calculated anomaly is again appreciably narrower than that predicted by Merkel and Alexander and the pull-up of the response directly over the body for larger dipole separations is also less pronounced. An estimate of the importance of the maximum response for  $\rho_m = \rho$  can be obtained from the plot of Figure 15 to be about 10% and 15% of the maximum response for  $\rho_m = 0.01 \rho$  and  $\rho_m = 0.1 \rho$ , respectively.

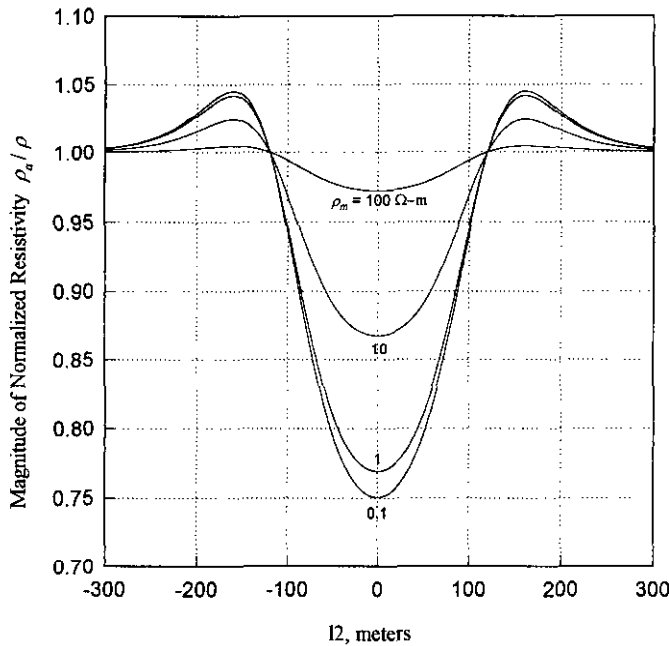


Fig. 11. Traverse directly over the prism of Figure 8 for various  $\rho_m$  at a frequency of 1 Hz; earth and prism relative permeability = 1.0,  $na = 3a = 180$  m.

**6. COLE-COLE RESISTIVITY FOR THE DEY AND MORRISON AND MERKEL AND ALEXANDER EXAMPLES**

Since the calculated  $\rho_a / \rho$  magnitudes for the above two examples are in reasonable accord with previous work when there is no induced polarization, modelling of induced polarization effects in the buried bodies has been attempted. Each of the above examples has been run for the following parameter set in the Cole-Cole model for the body resistivities:

- $\rho_m = 10$  ohm metres,
- $m_m = 0.25$ ,
- $\tau_m = 0.1$  seconds
- and
- $c_m = 0.5$ .

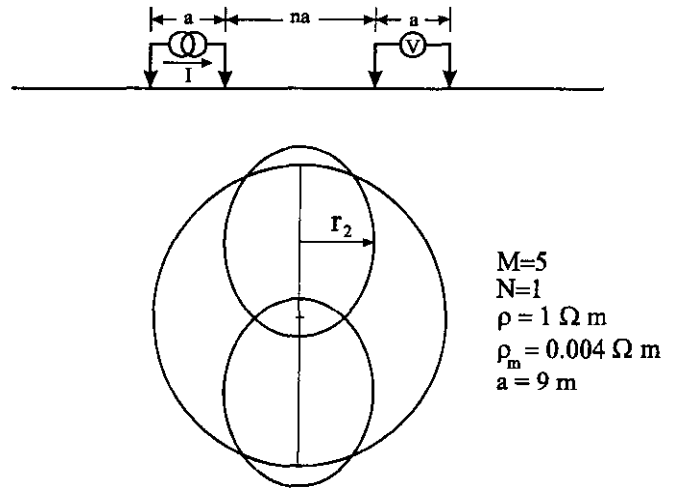


Fig. 12. The Merkel and Alexander (1971) example; M = 5, N = 1.

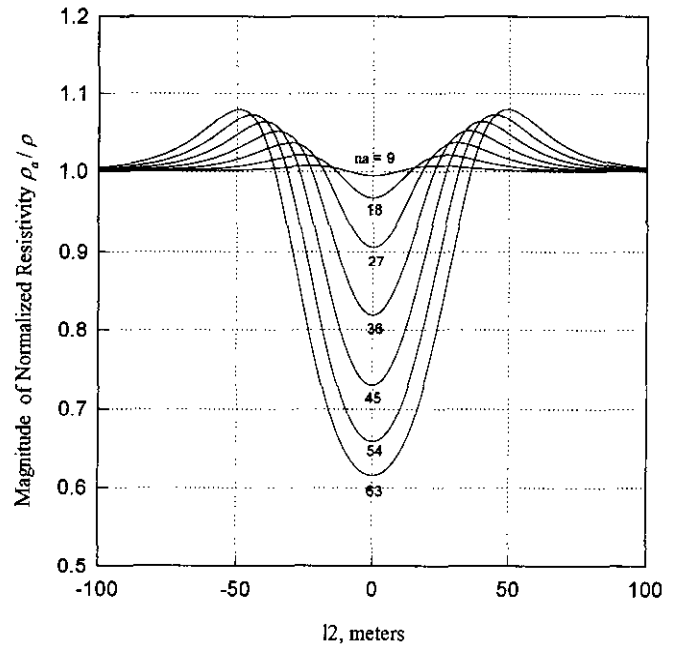


Fig. 13. Traverse directly over the Merkel and Alexander "sphere" model at a frequency of 1 Hz; earth and "sphere" relative permeability = 1.0.

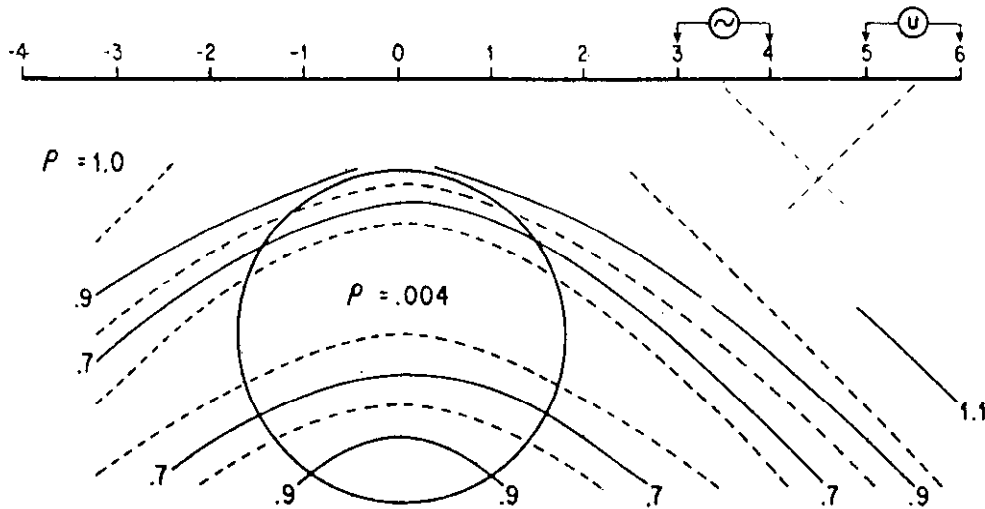


Fig. 14. Pseudosection for the Merkel and Alexander example.

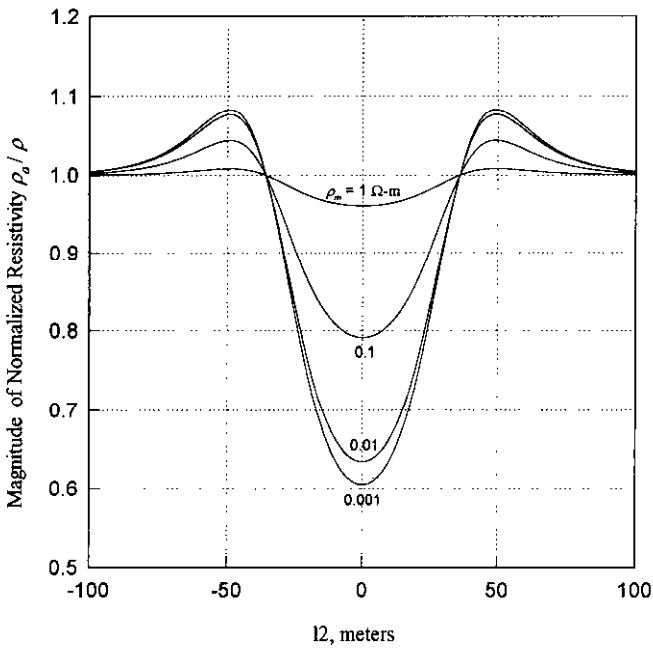


Fig. 15. Traverse directly over the "sphere" of Figure 12 for various values of  $\rho_m$  at a frequency of 1 Hz; earth and "sphere" relative permeability = 1.0,  $a = 9$  m,  $na = 7a = 63$  m.

The bodies were embedded in an earth with  $\rho = 100$  ohm metres,  $m = 0$  and traverses were run directly over them at a frequency of 1 Hz ( $na = 180$  metres for the Dey and Morrison example and  $na = 63$  metres for the Merkel and Alexander example) to compare the  $m_m = 0$  case to the  $m_m = 0.25$  case. Results of these traverses are given in Figures 16 and 17. In both cases, the effect of IP on the magnitude of  $\rho_a / \rho$  is small but the effect on the phase is substantial, as would be expected at a frequency of 1 Hz.

For the Merkel and Alexander example, propagation effects and EM coupling effects on  $\rho_a / \rho$  are small for  $m$  and  $m_m = 0$  at 1 Hz. Then, according to Seigel (1959), the phase  $\phi_{ma}$  of  $\rho_a / \rho$  when the resistivity of the body is described by

a Cole-Cole model should be given by

$$\phi_{ma} = \phi_m \frac{\partial \ln \rho_a}{\partial \ln \rho_m} \quad (2)$$

where  $\phi_m$  is the phase angle of resistivity of the body at the frequency under consideration. For the present situation, calculation of  $\rho_a$  for  $\rho_m = 10$  ohm metres and  $\rho_m = 20$  ohm metres to estimate the derivative in equation (2) yields

$$B_2 = \frac{\partial \ln \rho_a}{\partial \ln \rho_m} = 0.127.$$

The value of  $\phi_m$  at 1 Hz for the body Cole-Cole parameters in this example is -57 milliradians and this yields a value of  $\phi_{ma} = -7$  milliradians. If this is added to the phase of +1 milliradian for the  $m = m_m = 0$  case, the value of  $\phi_{ma}$  for  $m_m = 0.25$  is nearly the same as the -6 milliradians shown in Figure 17.

The Merkel and Alexander example with  $\rho = 100$  ohm metres and  $\rho_m = 20$  ohm metres also approximates the "2a" by "2a" cube buried "a" below the surface shown in Figure 3 of Hohmann (1975). The maximum value of  $B_2$ , expressed in percent, given by Hohmann is 14%, in reasonable agreement with the 11.4% calculated directly from the phase plot for the simulation of the "1.75a"-diameter Merkel and Alexander sphere used in this work.

### 7. CONCLUSIONS

A technique developed for dealing with the effect of buried cylindrical bodies on complex resistivity surveys has been shown to yield usable results for cylinders with length-to-diameter ratios as low as 3/2. In employing the technique, care must be exercised in interpreting data when the resistivity of the cylinder approaches that of the earth because there can be a significant response predicted when none should exist. The calculations can be carried out with ease and speed and the results can be displayed conveniently so that experimentation to determine the detectability of a body or experimentation to interpret field measurements is possible.

RESISTIVITY RESPONSE OF VERTICAL CYLINDER

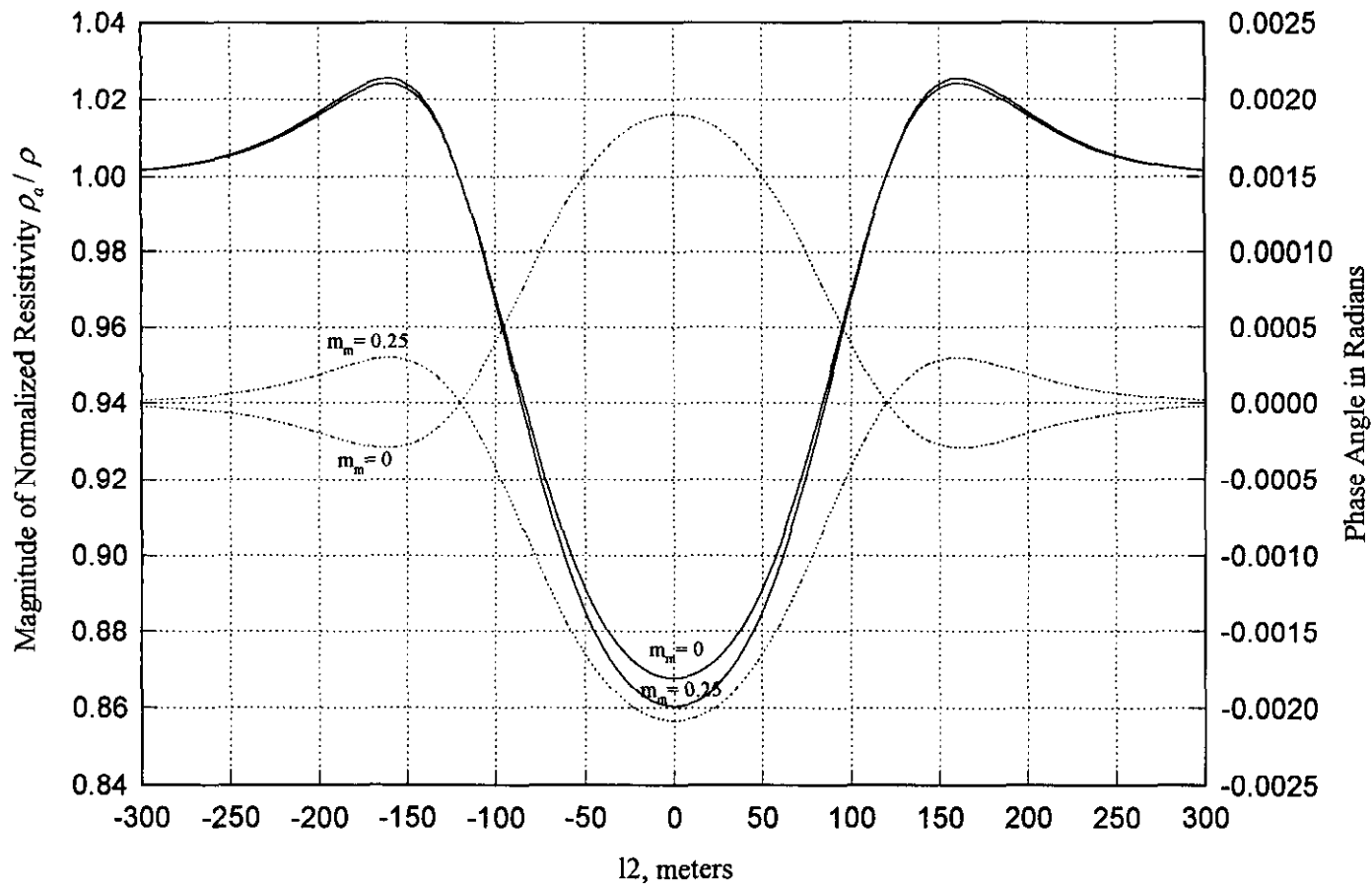


Fig. 16. Traverse directly over the Dey and Morrison prism at 1 Hz for  $\rho = 100$  ohm metres,  $m = 0$ ,  $\rho_m = 10$  ohm metres,  $m_m = 0.25$ ,  $\tau_m = 0.1$  seconds,  $c_m = 0.5$ ,  $a = 60$  m and  $na = 3a = 180$  m.

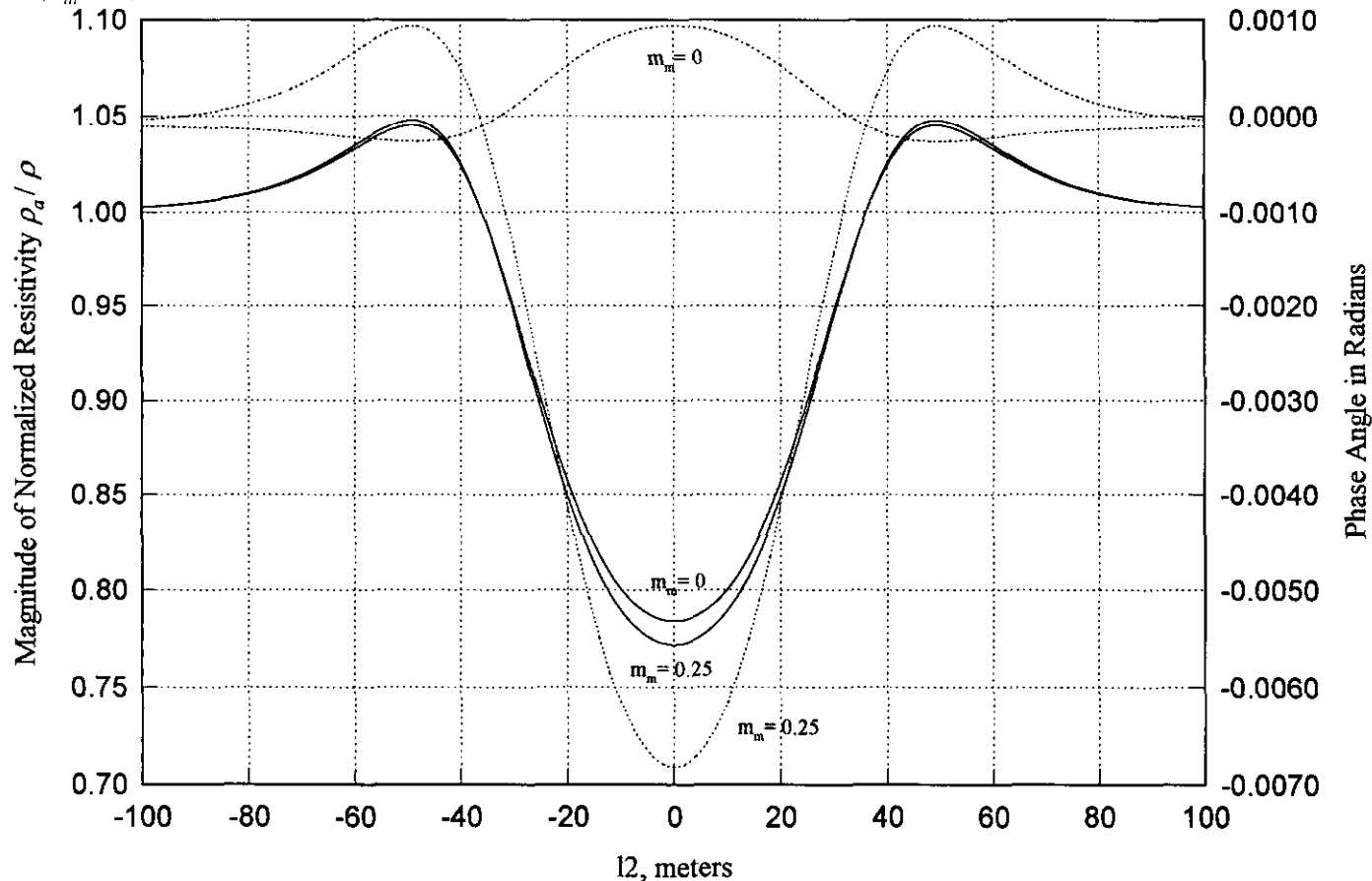


Fig. 17. Traverse directly over the Merkel and Alexander sphere at 1 Hz for  $\rho = 100$  ohm metres,  $m = 0$ ,  $\rho_m = 10$  ohm metres,  $m_m = 0.25$ ,  $\tau_m = 0.1$  seconds,  $c_m = 0.5$ ,  $a = 9$  m and  $na = 7a = 63$  m.

## REFERENCES

- Dey, A. and Morrison, H.F., 1979, Resistivity modelling for arbitrarily shaped three-dimensional structures: *Geophysics* **44**, 753-780.
- Hohmann, G.W., 1975, Three-dimensional induced polarization and electromagnetic modelling: *Geophysics* **40**, 309-324.
- Johnston, R.H., Trofimenkoff, F.N. and Haslett, J.W., 1987, Resistivity response of a homogeneous earth with a finite length contained vertical conductor: *Inst. Electr. Electron. Eng., Trans. Geosci. Remote Sensing* **GE-25**, 414-421.
- \_\_\_\_\_, \_\_\_\_\_, 1992, The complex resistivity response of a homogeneous earth with a finite length contained vertical conductor: *Inst. Electr. Electron. Eng., Trans. Geosci. Remote Sensing* **30**, 46-54.
- Macnae, J.C., 1979, Kimberlites and exploration geophysics: *Geophysics* **44**, 1395-1416.
- Merkel, R.H. and Alexander, S.S., 1971, Resistivity analysis for models of a sphere in a half-space with buried current sources: *Geophys. Prosp.* **19**, 640-651.
- Pelton, W.H., Sill, W.R. and Smith, B.D., 1983, Interpretation of complex resistivity and dielectric data, part I: *Geophys. Trans.* **29**, p. 297-330.
- Seigel, H.O., 1959, Mathematical formulation and type curves for induced polarization: *Geophysics* **24**, 547-565.
- Sternberg, B.K., 1991, A review of some experience with the induced-polarization/resistivity method for hydrocarbon surveys: successes and limitations: *Geophysics* **56**, 1522-1532.
- Trofimenkoff, F.N., Johnston, R.H., Haslett, J.W. and Klassen, A., 1993, Complex resistivity of a uniform earth in the presence of a well casing: 1993 Ann. Conv., Can. Soc. Expl. Geophys., Poster Presentation.
- Wait, J.R., 1982, *Geo-electromagnetism: Chapter 1*, Academic Press Inc.
- Williams, J.T. and Wait, J.R., 1985, EM and IP response of a steel well casing for a four-electrode surface array: Part I. Theory; Part II. Numerical results: *Geophys. Prosp.* **33**, 723-745.